11-2018

Investigation of carrier density and mobility variations in graphene caused by surface adsorbates

Hongmei Li
Clemson University, hongmel@g.clemson.edu

Xu Han
Clemson University

Anthony C. Childress
Clemson University

Apparao M. Rao
Clemson University

Goutam Koley
Clemson University

Investigation of carrier density and mobility variations in graphene caused by surface adsorbates

Hongmei Li[1], Xu Han[1,3], Anthony S. Childress[2], Apparao M. Rao[2] and Goutam Koley[1]

[1] Department of Electrical and Computer Engineering, Clemson University, SC 29625, USA
[2] Department of Physics and Astronomy, Clemson University, SC 29625, USA
[3] Department of Electrical and Computer Engineering, Old dominion University, VA 23505, USA

E-mail: hongmel@clemson.edu

Abstract

Conductivity, carrier concentration and carrier mobility in graphene were investigated as a function of time in response to ionized donor and acceptor adsorbates. While a reduction in conductivity and hole density in graphene was observed upon exposure to a weak electron donor NH_3, the carrier mobility was found to increase monotonically. The opposite behavior is observed upon exposure to NO_2, which is expected based on its typical electron withdrawing property. Upon exposure to $C_9H_{22}N_2$, a strong donor, it resulted in the transformation of graphene from p-type to n-type, although the inverse variation of carrier concentration and mobility was still observed. The variational trends remained unaltered even after intentional introduction of defects in graphene through exposure to oxygen plasma. The responses to $C_9H_{22}N_2$, NH_3 and NO_2 exposures underline a strong influence by ionized surface adsorbates, that we explained via a simple model considering charged impurity scattering of carriers in graphene.

Keywords: graphene, graphene mobility, carrier density, NH3, NO2, gas molecule adsorption

1. Introduction

Since the first discovery of the Graphene in 2004, extensive research has been carried out worldwide to investigate its unique material properties and device applications [1-5]. Among the numerous potential applications of graphene reported [6-7], inexpensive yet high performance sensor development has emerged as one of the most attractive fields in terms of practical applicability in the short term. There are several unique attributes of graphene, such as high surface-to-volume ratio, high carrier mobility, and unsaturated sp^2 bonds, which make it very appealing for sensing applications [8]. Although numerous reports on graphene's excellent sensing behavior exist, there are many instances where the sensing mechanism is not completely understood [9]. For example, while many sensing applications are based on the change in conductivity or Dirac point in graphene, measured in various device configurations (resistor, FET, Schottky diode), and/or with functionalization layers (Pd, Pt, Au), those simple measurements are not sufficient to provide a detailed understanding of the sensing mechanisms in graphene [10-13]. This is because conductivity is proportional to the product of two basic charge carrier properties, mobility and concentration, so information regarding the change in conductivity (due to molecular adsorption) does not offer insight into their individual changes. On the other hand, measurement of Dirac point shift directly correlates with changes in charge density in graphene, but does not provide information on the change in mobility. Mobility and carrier concentration can change independently of one another depending on the characteristics of the adsorbing molecules, and knowledge of the change in both parameters (especially with time dependence) can be helpful in determining the type of the molecules adsorbed.

One way to independently determine the variation in mobility and conductivity caused by molecular adsorption is by fabricating a graphene based field effect transistor in a back-gated configuration [10,14]. This allows one to extract the conductance (σ) and transconductance (g_m) from the $I_d - V_d$ and the $I_d - V_g$ plots, respectively, which can then be used to find the field effect mobility and the carrier concentration (please refer to appropriate formulas and discussion below). However, a high back gate voltage may be required to obtain an appreciable change in I_d (or more preferably the "V-shaped"

characteristics), depending on the insulator (typically SiO_2) thickness and the carrier density in graphene, which may also cause the insulator to leak and even breakdown. Even if the insulator does not break, there is always a chance of charge injection and accumulation in the insulator layer, causing the slope of the $I_d - V_g$ characteristics to be altered leading to an erroneous determination of mobility. Additionally, this technique only works when it is possible to use a back gate (or a top gate, which is more cumbersome to realize), and is not suitable for graphene transferred to arbitrary substrates. An alternative technique to simultaneously determine changes in carrier mobility and concentration in graphene transferred onto an arbitrary non-conductive substrate is based on Hall Effect measurement. At low magnetic fields, and in the presence of a majority carrier (away from the Dirac point) in graphene, this is a reliable technique to independently and simultaneously measure carrier mobility and concentration.

In this article, we report on simultaneous measurements of temporal variations in carrier mobility and carrier concentration caused by molecular adsorption on graphene, systematically for the first time, using Hall effect measurements. Graphene was exposed to two different types of gas molecules, NH_3 and NO_2, which typically behave as donors and acceptors in graphene. It was observed that exposure to the gases changed the conductivity in opposite directions, as expected; however, the temporal variations in carrier concentration and mobility were found to be intriguing. A simple physical model has been proposed to explain the observations. Effect of heavier doping, through exposure to an organic chemical (trimethylhexamethylenediamine ($C_9H_{22}N_2$)) carrying two amine groups, was also investigated, which first reduced the carrier concentration and then flipped the doping of graphene from p-type to n-type, which eventually recovered close to the initial doping level upon removal of the exposure.

2. Experimental section

The graphene used in this study was synthesized on copper foils using a home-built chemical vapor deposition (CVD) system, then cut to 6 × 6 mm square shapes to transfer on thermally grown 300 nm SiO_2/Si (n^+) substrates. Detailed growth conditions and process steps have been described in the previous report [14]. To examine the quality of the graphene, Raman spectra (Renishaw Raman system, InVia., 532 nm) and atomic force microscope (AFM) images (Veeco 3100) were recorded. Field effect mobility and carrier concentration were also determined by fabricating devices in a back-gated FET configuration by depositing source and drain ohmic contact metal stacks of Au (80 nm)/Ti (20 nm) on the graphene, and the highly doped n-Si substrate working as the back gate. The carrier mobility and concentration were also separately determined from Hall Effect measurements. For this, pressed Ohmic contacts using In/Sn alloy dots (95%-In, 5%-Sn) were formed at four corners of a square shaped graphene layer (on a SiO_2/Si substrate), and the mobility (μ_{Hall}), sheet carrier concentration (n_{Hall}) and conductivity (σ_{Hall}) were obtained with an Ecopia HMS 3000 system. To simultaneously measure the carrier density and mobility during gaseous exposure, a quarter inch flow tube was connected to the chamber where the sample is loaded (and exposed to a 0.55 T magnetic field) during probing as shown in the schematic in Fig. 1. Two high purity (99.999 %) calibrated gases from Praxair Inc., 475 ppm NH_3 and 5 ppm NO_2 (both diluted in N_2) were used for the gas sensing experiments.

3. Results and Discussion

3.1 Graphene characterization

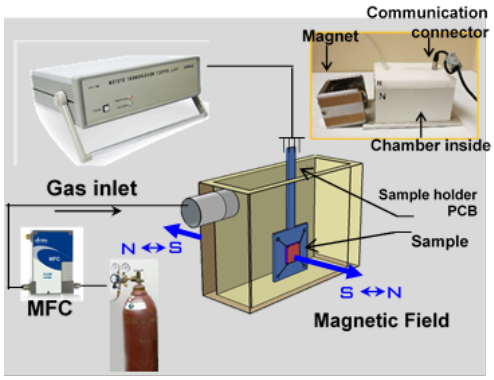

Figure 1. Schematic diagram of the Hall measurement apparatus. The test sample was placed in the closed measurement chamber fitted with a gas inlet. A mass flow controller was used to control and switch the flow of test gases, NH_3 (475 ppm) / NO_2 (5 ppm), flow ON and OFF. Inset at the top right shows a picture of the actual measurement chamber and 0.55 T magnet of the Hall measurement system.

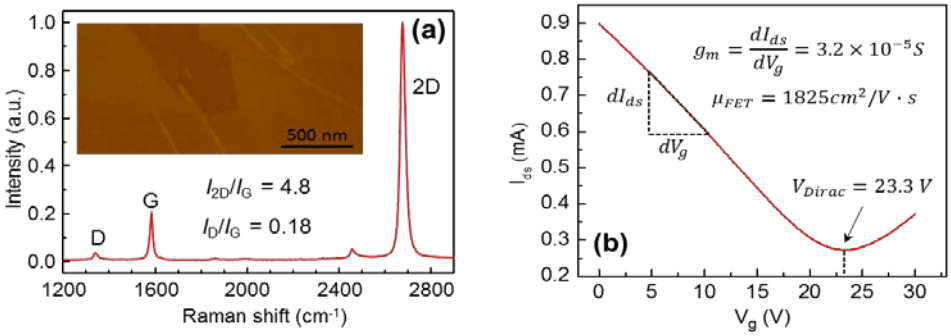

Figure 2. a) Raman spectra of graphene transferred to SiO_2/Si substrate showing low defect and monolayer nature. The inset shows a 4 × 2 µm AFM image of the graphene with a smooth surface and a few wrinkles that are typically formed during transfer. b) I_{ds} – V_g characteristic measured from back-gated graphene FET device showing typical V-shaped characteristic. A Dirac point of 23.3 V indicates p-type nature.

A typical Raman spectrum taken on graphene transferred to SiO_2/Si substrate is shown in Fig. 2(a). Graphene's characteristic peaks *G*, *D* and *2D* are marked in the Raman spectrum, and their intensity ratios are calculated as I_{2D}/I_G = 4.8, I_D/I_G = 0.18, indicating high quality monolayer graphene [15]. Inset of the Fig. 2(a) is a graphene's AFM image showing smooth morphology with a few wrinkles as typically observed in high quality transferred graphene. Representative I_{ds} – V_g characteristics measured from a back gated graphene FET device is shown in Fig. 2(b). The positively shifted Dirac point at ~23.3 V indicates the graphene is p-type, which is expected for graphene transferred on SiO_2 substrates [16-17]. From the I_{ds} – V_g, plot, the transconductance $g_m = \partial I_{ds}/\partial V_g$ is calculated (see dotted straight line in the p-type region of the curve) to be 3.2 × 10^{-5} S. Using the relationship $\mu_{FE} = g_m L/(WC_{ox}V_{ds})$ (C_{ox} is the gate oxide capacitance, G is the conductance, L and W are the material's length and width between source and drain, respectively) [14], the field effect mobility (μ_{FE}) can be calculated to be 1,825 $cm^2V^{-1}s^{-1}$ (Fig.2(b)).

3.2 Response to NH_3 and NO_2 gas molecules

To investigate the adsorption induced property changes in graphene it was exposed to typical electron donating NH_3 (475 ppm) gas and electron withdrawing NO_2 (5 ppm) gas, and the carrier density and mobility changes were recorded as a function of time using Hall measurements. First, NH_3 gas was introduced into the chamber at a constant flow rate of 50 sccm for 65 min until the electron density and mobility reached steady state values. Then the sample was taken out of the chamber, and left to recover in ambient air for over 2 hours. Throughout the exposure and recovery processes, conductivity (σ_{Hall}), carrier density (n_{Hall}) and mobility (μ_{Hall}) measurements were conducted consistently at intervals of 10 – 30 minutes. On the plots in Fig. 3(a), the left axes show the measured values for each parameter, while the right axes show percentage changes. From the plot, we find that the conductivity and carrier concentration monotonically decreases with time of exposure, and reaches values that are ~30% and ~50% lower than the pre-exposure values, respectively. Since the NH_3 molecule contains NH_2 (amine) group, which

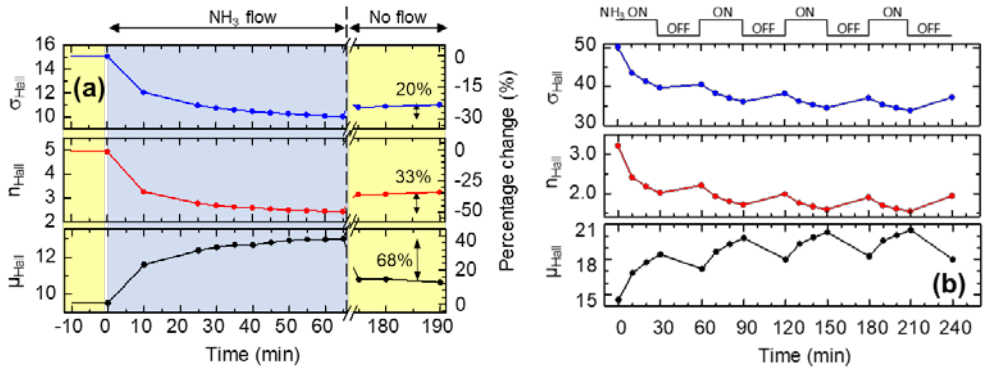

Figure 3. Temporal variation in conductivity (σ_{Hall} / 10^2 $\Omega^{-1}cm^{-1}$), carrier mobility (μ_{Hall} / 10^2 $cm^2V^{-1}s^{-1}$) and density (n_{Hall} / $10^{12}cm^{-2}$) recorded in response to switching ON and OFF of 475 ppm NH_3 gas flow. a) The gas was flown until their steady state values were reached, followed by recovery in ambient (out of the chamber) for over 2 hours. The left axes show the actual measured value for each parameter, while the right axes show the corresponding percentage change. b) Variation in conductivity (σ_{Hall} / 10^2 $\Omega^{-1}cm^{-1}$), carrier mobility (μ_{Hall} / 10^2 $cm^2V^{-1}s^{-1}$) and density (n_{Hall} / $10^{12}cm^{-2}$) to 4 cycles of NH_3 gas exposure (30 mins) alternating with periods of recovery (30 mins).

is highly electron donating in nature, its adsorption on graphene (originally p-type) upon exposure results in n-type doping [18] and consequent reduction in hole concentration. In contrast to the conductivity and carrier concentration, the mobility increases with the duration of NH_3 exposure. This is contrary to the normal expectation that charged impurities, no matter the nature, would always result in a reduction of the carrier mobility due to enhanced scattering effect. Response to periodic (alternate switching on and off of the gas flow every 30 mins) NH_3 exposure to graphene was further studied, and the results are shown in Fig. 3(b). Once again the conductivity (σ_{Hall}), sheet carrier concentration (n_{Hall}) changed in similar fashion while the Hall mobility (μ_{Hall}) behaved differently.

To investigate the response caused by the adsorption of electron withdrawing molecules, we exposed the graphene sample to 5 ppm NO_2 in the same Hall measurement setup. The temporal variations in conductivity, carrier mobility and concentrations are shown in Fig. 4. As expected, the carrier concentration (hole) increased upon exposure to NO_2, which is caused by their electron withdrawal nature. The conductivity also increased, however, the mobility showed a decreasing trend. Interestingly, even after stopping the gas flow over 2 hours, the properties of the graphene did not recover, unlike the NH_3 case. This is likely due to the higher adsorption binding energy (by a factor of 2 – 4) of NO_2 compared to NH_3, which results in its desorption rate being much slower [19]. To facilitate general comparison with other gas sensing results in the literature [20 – 22] that often shows the response in Dirac point as a function of time (upon gaseous exposure), we calculated graphene's Dirac point shift due to molecular doping by NH_3 or NO_2 using the correlation between carrier density change Δn and Dirac point shift ΔV_{Dirac}, given as: $\Delta V_{Dirac} = (\Delta n \cdot q \cdot t_{ox}) / \varepsilon\varepsilon_0$ [20], where q is the electron charge, t_{ox} is the SiO_2 thickness (100 nm), ε and ε_0 are the dielectric constant of SiO_2 and vacuum permittivity, respectively. After NH_3 and NO_2 gas exposure for 50 minutes, graphene's Dirac point shifts are calculated to be ~-11 V and ~3 V, respectively, using the above equation (which of course can also be used to plot the Dirac point shifts as a function of time from the Δn variations). The direction of Dirac point shifts upon NH_3 and NO_2 gas exposures are as expected, since the electron donating nature of the former reduces the Dirac point, while the electron withdrawing nature of the latter does the opposite. The magnitude of Dirac point shifts are also in agreement to those reported by Singh et. al [20] (-6 V and -8 V, respectively for similar concentrations of NH_3 and NO_2) measured directly in a back-gated FET configuration with the same SiO_2 thickness.

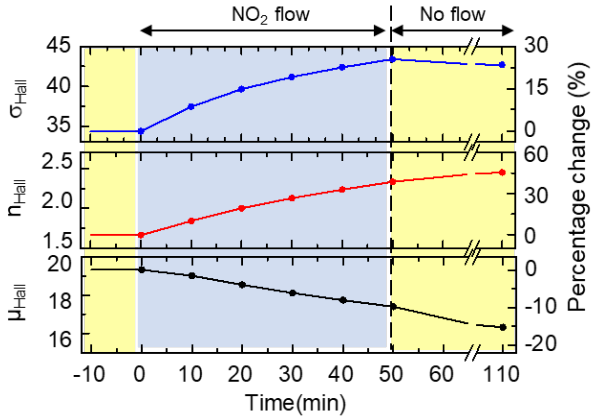

Figure 4. Temporal variation in conductivity (σ_{Hall} / 10^2 $\Omega^{-1}cm^{-1}$), carrier mobility (μ_{Hall} / 10^2 $cm^2V^{-1}s^{-1}$) and density (n_{Hall} / $10^{12}cm^{-2}$) recorded in response to switching ON and OFF of 5 ppm NO_2 gas flow. The gas was flown for 50 mins followed by recovery in ambient (out of the chamber) for over 1 h. The left axes show the actual measured value for each parameter, while the right axes show the coresponding percentage change.

From Figs. 3 and 4, we note that the adsorption of NO_2 reduces carrier mobility in graphene, while NH_3 results in an increase. Clearly, the charge on the adsorbed molecules is affecting the mobility. Indeed, it is commonly accepted that the carrier mobility in graphene transferred to SiO_2 is strongly affected by long-range scattering from charged impurities near graphene or trapped at the interface of graphene/SiO_2 (graphene on the SiO_2 substrate participates in a redox reaction that takes place with molecules adsorbed from ambient environment following: $O_2 + 2H_2O + 4e^-$ (from graphene) = $4OH^-$) [16, 23-25]. It is, therefore, reasonable to expect that the charged gas molecules adsorbed on the graphene's surface (after transferred the charge to the graphene) would act as scattering centers affecting the carrier mobility. However, it is interesting to note that the mobility increases as the surface density of positively charged NH_3 molecules increases, and decreases as the negatively charged NO_2 molecular density increases. We propose a simple explanation for this observation considering that the carrier mobility in graphene is affected by an interaction between the following quantities: (i) the total charge density near the graphene surface or on the SiO_2 substrate (σ_{sub}), (ii) the graphene's charge carrier density (n_s), and (iii) density of ionized gas molecules (σ_{mol}) adsorbed on graphene. The addition of positively charged NH_3 ions on the surface screens the effect of net negative charge

surrounding graphene (which gives rise to its p-type behavior), hence enhances the carrier mobility. On the other hand, the addition of negatively charged NO_2 ions on the surface enhances the electrostatic interaction of the already existing net negative charge around graphene, and enhances scattering. Figures 5(a) and (b) shows arrays of electrostatic charges σ_{sub}, n_s and σ_{mol} where the charges on adsorbed NH_3 and NO_2 molecules can reduce or enhance the scattering effect of pre-existing (mostly substrate) charges surrounding graphene.

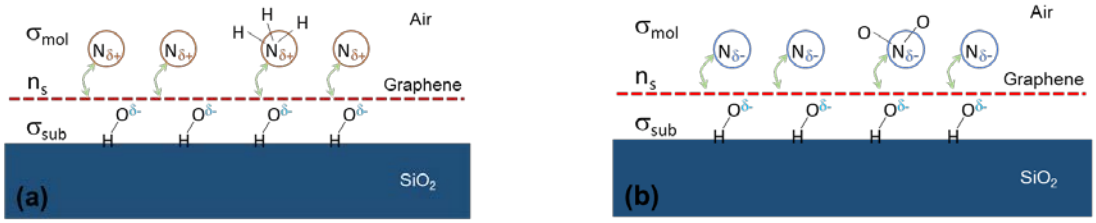

Figure 5. Schematic diagram showing electrostatic charge distribution with ionized (a) NH_3 and (b) NO_2, ionized adsorbates, respectively. Pre-existing charged impurities from the interface and substrate (σ_{sub}), the graphene carrier density (n_s), and the charged gas molecules (σ_{mol}) on graphene surface are shown.

The effect of adsorbate charge and dipole moment on screening the effect of scattering electric field from surrounding charges in graphene has been theoretically modelled by Liang, *et al*. (*Phys. Rev. B*, 2014) [26]. They found that indeed adsorbate charge or dipole moments can significantly screen the effect of pre-existing charged impurities. However, their work (or any other work to the best of our knowledge) did not investigate the mobility change directly (instead, focusing on conductivity variation) and independently, or compared with experimental results. Additionally, their model is limited to considering only dipolar interaction from NH_3 and NO_2 adsorbates (so that charge density remains constant), which is directly contradicted by our experimental findings of both conductivity and mobility variations.

3.3 Response to strong donor type molecules

To further verify our above observations and assertions, we exposed graphene to a much stronger electron donor (than NH_3) trimethylhexamethylenediamine ($C_9H_{22}N_2$), which has two electron donating functional amine groups (its chemical structure is shown in the inset of Fig. 6). The idea was to surface dope the normally p-type graphene so strongly n-type that it is transformed to an n-type graphene, which offers the opportunity to the study of the electrical parameter variations and their inter-correlations, as a function of time, as the transformation happens [10]. The graphene sample (transferred to a Si/SiO_2 substrate like other discussed above) was exposed to $C_9H_{22}N_2$ vapor by putting a drop in its close proximity, which was followed by measurement of conductivity, mobility and carrier concentration as a function of time approximately 10 mins after exposure. From Fig. 6, we find that the exposure started reducing the hole density of graphene quickly, which kept dropping and until after ~30 minutes when the graphene switched over from p- to n-type. It is important to note that when the graphene was still p-type, the carrier density and mobility changed in a way similar to what we saw with NH_3 gas exposure i.e. the mobility increased while the carrier density (hole) reduced. After the graphene changed to n-type, and the adsorbed molecules started to

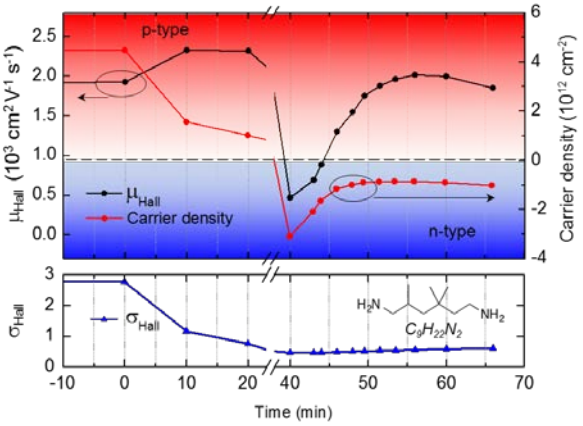

Figure 6. Temporal variation in conductivity (σ_{Hall} / 10^2 $\Omega^{-1}cm^{-1}$), carrier mobility (μ_{Hall} / 10^2 $cm^2V^{-1}s^{-1}$) and density (n_{Hall} / $10^{12}cm^{-2}$) recorded in response to exposure to trimethylhexamethylenediamine ($C_9H_{22}N_2$). The top graph shows carrier concentration (n_{Hall}) and Hall mobility (μ_{Hall}) variations, while the bottom one depicts changes in conductivity (σ_{Hall} / 10^2 $\Omega^{-1}cm^{-1}$).

desorb, the same trend of mobility and carrier density variation was observed. In this case the electron is the majority carrier, and when the electron density was reduced, the mobility increased. It should be noted that this trend has been exhibited for all the three exposures considered in this study, i.e. increase in majority carrier density leads to a strong decrease in mobility, which clearly indicates ionized impurity scattering as a major factor limiting mobility in these devices, which is commonly observed [25,27]. With mobility increasing more rapidly than the decrease in carrier concentration, the conductivity has a slightly increasing trend, contrary to expectations and observations for NO_2 and NH_3. This exception, however, underscores that the carrier transport properties of electrons and holes in graphene, in response to ionized surface adsorbates, cannot be presumed to follow a simple trend, as has often been assumed in the past; and future sensor development or theoretical modeling efforts must take into account the independent variations of these parameters to gain a deeper understanding of the transport phenomena and benefit from it.

3.4 Response of defective graphene

Since graphene transferred to various substrates can be defective to different degrees, it is useful to investigate the effect of ionic adsorbates on the carrier transport properties of graphene with intentionally introduced defects, and see if the above trends still hold true. To this end, we exposed graphene to oxygen plasma (PE25-JW, Plasma Etch, Inc) for 2 s using a power setting at 25% and O_2 flow rate of 15 sccm. The Hall mobility was measured before and after plasma exposure, and was found to be dramatically reduced from 1150 to 360 $cm^2V^{-1}s^{-1}$, while the Hall carrier concentration was increased from 6.5 $\times 10^{12}$ to 8.2 $\times 10^{12}$ cm^{-2}. This is expected, however, since the introduction of structural defects upon O_2 plasma treatment (as verified through Raman measurements) to the graphene crystalline structure will create more open bonds and trapping sites, which can hold charge, as well as enhance interactions with gaseous molecules such as NH_3, causing more charge exchange and enhanced scattering of the carriers [28, 29]. Evidence of such charging is found in the increased carrier (hole) concentration, which indicates electrons are being trapped by the opened bonds, which also likely contributed to more scattering and consequent reduction in carrier mobility. Although the exact mechanisms for such trapping and molecular interaction is not clear to us at this point, the significant role of plasma treatment in affecting graphene's electronic and sensing properties (see below) is clearly evident.

The response to NH_3 gas exposure was studied, before and after the oxygen plasma treatment, to determine the graphene response to the introduction of defects. The results are shown in Fig. 7 which shows plots of Hall mobility and concentration vs. time as 475 ppm NH_3 gas flow was switched on and off. From Fig. 7, we find that the plasma treated defective graphene shows much higher sensitivity and faster response time (~50 % change in 10 mins compared to ~18% change in 40 mins) compared to untreated graphene. This is an interesting result from the point of view of sensor development indicating that the open bonds and raised carrier concentration as a result of plasma treatment can provide more interaction opportunity for the NH_3 molecules, which produces a higher magnitude of response at a faster rate. This observation is also in line with the prior observation of higher sensing response for more defective graphene [30]. Although the magnitude and rate of response were

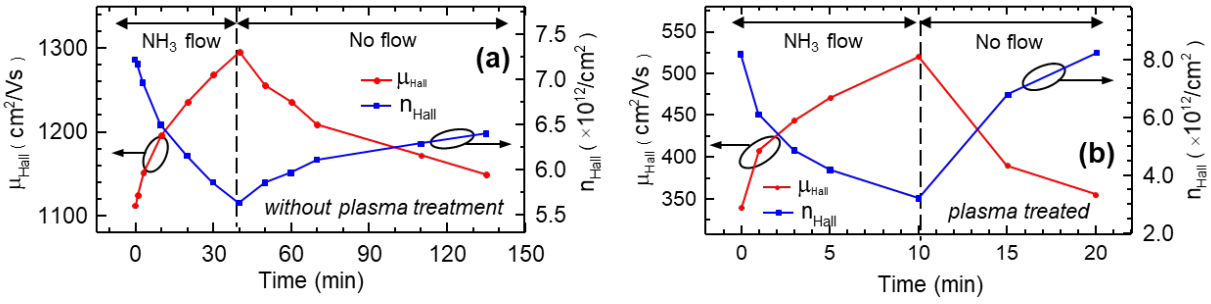

Figure 7. O_2 plasma treatment effects on graphene responses to NH_3 gas. Temporal variation in graphene carrier mobility and density (a) before O_2 plasma treatment and (b) after O_2 plasma treatment.

different, the overall trend of the mobility and carrier concentration change due to NH_3 exposure remained very similar, underscoring the validity of the proposed model even for highly defective graphene.

4. Conclusion

In summary, we have reported, for the first time, on individual variations in conductivity, mobility and carrier concentration of graphene under the effect of NH_3 and NO_2 gases and $C_9H_{22}N_2$ vapor exposure, using Hall measurement techniques. It was observed in all three cases of exposure, involving an acceptor (NO_2), a weak (NH_3) and a strong donor ($C_9H_{22}N_2$) that a reduction in majority carrier density resulted in an increase in mobility, and vice-versa, regardless of the type of carriers, as expected for ionized impurity dominated carrier transport. Exposure of p-type graphene to electron donating NH_3 resulted in

the screening of negatively charged pre-existing impurities around graphene, resulting in an increase in carrier mobility associated with a reduction in p-type carrier density. On the other hand, exposure to electron withdrawing NO_2 caused a decrease in carrier mobility with an accompanying increase in carrier density. Exposure to a strong electron donor $C_9H_{22}N_2$ resulted in transformation of p-type graphene to n-type, with an increasing trend in mobility observed for both n-type and p-type phases as the carrier density reduced. Such trends were also found to be valid for intentionally defect introduced graphene, although the magnitude and rate of changes varied significantly. Our observations clearly underline the importance of independent determination of carrier mobility and density, and their impact on understanding transport in graphene, especially in the presence of ionic adsorbates.

Acknowledgements

Financial support for this work from the National Science Foundation (Grants Nos. IIP-1512342, CBET-1606882, IIP-1602006, and EEC-1560070) is thankfully acknowledged.

References

[1] Allen M J, Tung V C, and Kaner R B 2009 *Chem. Rev*. **110 [1]** 132
[2] Shao Y, Wang J, Wu H, Liu J, Aksay I A and Lin Y 2010 *Electroanalysis*. **22[10]** 1027
[3] Young R J, Kinloch I A, Gong L and Novoselov K S 2012 *Compos. Sci. Technol.* **72 [2]** 1459
[4] Li X, Rui M, Song J, Shen Z and Zeng H 2015 *Adv. Funct. Mater*. **25 [31]** 4929
[5] Zhou X, Qiao J, Yang L and Zhang J 2014 *Adv. Energy Mater*. **4** 8
[6] Choi W, Lahiri I, Seelaboyina R and Kang Y S 2010 *Crit. Rev. Solid State Mater. Sci*. **35 [1]** 52
[7] Liu J, Liu Z, Barrow C J and Yang W 2015 *Anal. Chim. Acta.* **859** 1
[8] Schedin F, Geim A K, Morozov S V, Hill E W, Blake P, Katsnelson M I and Novoselov K S 2007 *Nat. Mater*. **6** 652
[9] Basu S and Bhattacharyya P 2012 *Sens. Actuators, B.* **173** 1
[10] Uddin M A, Zhu Y, Singh A, Li H, Islam M S and Koley G 2016 *J. Phys. D: Appl. Phys*. **49** 46LT02
[11] Singh A, Uddin M, Sudarshan T and Koley G 2014 *Small*. **10** [8], 1555
[12] Uddin M A, Singh A, Daniels K, Vogt T, Chandrashekhar M V S, and Koley G 2016 *Jpn. J. Appl. Phys*. **55** 110312
[13] Gautam M and Jayatissa A H 2012 *J. Appl. Phys*. **111**, 094317
[14] Li H, Zhu Y, Islam M S, Rahman M A, Walsh K B and Koley G 2017 *Sens. Actuators, B.* **253** 759
[15] Ferrari A C 2007 *Solid State Commun*. **143 [1-2]** 47
[16] Xu H, Chen Y, Zhang J and Zhang H 2012 *Small*. **8 [18]** 2833
[17] Ishigami M, Chen J H, Cullen W G, Fuhrer M S and Williams E D 2007 *Nano Lett*. **7** [6] 1643
[18] Morokuma K 1977 *Acc. Chem. Res*. **10 [8]** 294
[19] Leenaerts O, Partoens B and Peeters F M 2008 *Phys. Rev. B*. **77** 125416
[20] Singh A K, Uddin M A, Tolson J T, Maire-Afeli H, Sbrockey N, Tompa G S, Spencer M G, Vogt T, Sudarshan T S and Koley G 2013 *Appl. Phys. Lett*. **102 [4]** 043101
[21] Nomani M W, Shields V, Tompa G, Sbrockey N, Spencer M G, Webb R A and Koley G. 2012 *Appl Phys. Lett.* **100 [9]** 092113
[22] Novoselov K S, Geim A K, Morozov S V, Jiang D A, Zhang Y, Dubonos S V, Grigorieva I V, Firsov A A 2004 *Science*. **306** 666
[23] Van der Pauw L J 1958 *Philips Res. Rep*. **13** 1
[24] Adam S, Hwang E H, Galitski V M and Sarma S D 2007 *Proc. Natl. Acad. Sci*. **104** [47] 18392
[25] Chen J H, Jang C, Xiao S, Ishigami M and Fuhrer M S 2008 *Nat. Nanotechnol*. **3** [4] 209
[26] Liang S Z, Chen G, Harutyunyan A R and Sofo J O 2014 *Phys. Rev. B* **90** 115410
[27] Mach J, Procházka P, Bartošík M, Nezval D, Piastek J, Hulva J, Švarc V, Konečný M, Kormoš L and Šikola T 2017 *Nanotechnol*. **28** 415203
[28] Nourbakhsh A, Cantoro M, Vosch T, Pourtois G, Clemente F, van der Veen M H, Hofkens J, Heyns M M, De Gendt S and Sels B F 2010 *Nanotechnol*. **21** 435203
[29] Childres I, Jauregui L A, Tian J and Chen Y P 2011 *New J. Phys* **13** 025008
[30] Dan Y, Lu Y, Kybert N J, Luo Z and Johnson A C 2009 *Nano Lett.* **9** 1472